

Showcasing research from groups at the “Petru Poni” Institute of Macromolecular Chemistry, Laboratoire National des Champs Magnétiques Intenses-CNRS, Palacký University of Olomouc and University of Vienna

An iron(III)-centred ferric wheel  $\text{Fe}-(\text{Fe}_6)$  with a siloxane-based bis-salicylidene Schiff base

A salen-type Schiff base proved to be a powerful tool for assembly of a  $\{\text{Fe}_6\}$  wheel, in the centre of which a seventh iron(III) atom is hosted, providing the opportunity to vary the metal ions inserted in the wheel.

As featured in:



See Sergiu Shova, Vladimir B. Arion *et al.*, *Dalton Trans.*, 2017, 46, 1789.

Cite this: *Dalton Trans.*, 2017, **46**, 1789

Received 13th January 2017,

Accepted 18th January 2017

DOI: 10.1039/c7dt00141j

rsc.li/dalton

# An iron(III)-centred ferric wheel $\text{Fe}_7\{\text{Fe}_6\}$ with a siloxane-based bis-salicylidene Schiff base†

Sergiu Shova,<sup>a</sup> Maria Cazacu,<sup>a</sup> Ghenadie Novitchi,<sup>b</sup> Giorgio Zoppellaro,<sup>c</sup> Cyrille Train<sup>b</sup> and Vladimir B. Arion<sup>\*d</sup>

A new iron(III)-centred ferric wheel  $\text{Fe}_7\{\text{Fe}_6\}$  of the formula  $[\text{Fe}_7(\text{H}_2\text{L})_6(\text{NCS})_6](\text{ClO}_4)_3 \cdot 10\text{H}_2\text{O}$ , where  $\text{H}_4\text{L} = N,N'$ -bis(3-carboxylsalicylidene)-1,3-bis(3-aminopropyl)tetramethyldisiloxane, was synthesised and fully characterised.  $^{57}\text{Fe}$  Mössbauer spectra indicate the presence of high spin ( $S = 5/2$ )  $\text{Fe}^{3+}$  cations adopting a slightly different coordination environment in agreement with the X-ray diffraction structure. There are competing antiferromagnetic exchange interactions along the rim ( $J_1 = -1.00 \text{ cm}^{-1}$ ) and the radius ( $J_2 = -1.46 \text{ cm}^{-1}$ ) of the wheel.

## Introduction

$[\text{Fe}(\text{OME})_2(\text{O}_2\text{CCH}_2\text{Cl})]_{10}$  was the first isolated and well-characterised multinuclear iron(III) complex, with a nearly perfect cyclic structure referred to as a molecular ferric wheel.<sup>1</sup> Since then the number of these beautiful molecules has increased steadily to form one of the largest families of well-documented molecular wheels. The majority of them are even-numbered wheels with nuclearities including 6,<sup>2</sup> 8,<sup>3</sup> 10,<sup>1,3c,4</sup> 12,<sup>5</sup> 16<sup>3a</sup> and 18,<sup>6</sup> and only a very few examples of odd-numbered wheels (e.g., 9)<sup>7</sup> are known. Structurally more complex polynuclear aggregates with wheel-like motifs have been reported as well.<sup>8</sup> Although some level of control of the wheel size can be achieved in particular cases by using alkali metal ions as the template,<sup>9</sup> the synthesis of new wheel-architectures remains basically unanticipated, and an escape from serendipity to rational design and synthesis of molecular wheels is still an aim to be achieved. As the main building blocks for the synthesis of ferric wheels carboxylic acids and tripodal ligands, combining specific rigid groups and certain flexibility, are usually employed. First examples of using Schiff base ligands (e.g., 5-bromo-3-methoxysalicylideneaminoethanol and 3-(3-methoxysalicylidene-amino)benzyl alcohol) for assembly of

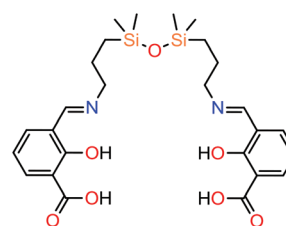


Fig. 1 Line drawing of the Schiff base  $\text{H}_4\text{L}$  prepared *in situ*.

carboxylate-free ferric wheels<sup>9,3e</sup> and ferrous disk shaped  $\{\text{Fe}\}_7$  aggregates<sup>10</sup> have been recently reported. To assess the generality of the assembly process, we propose to explore the use of a siloxane-bridged Schiff base<sup>11</sup> to synthesise ferric wheels. Herein we report the synthesis of a  $\{\text{Fe}\}_6$  molecular wheel which accommodates a seventh ferric ion into its  $\text{O}_6$ -wheel cavity starting from a Schiff base resulting from a 2 : 1 condensation of 3-formylsalicylic acid with 1,3-bis(3-aminopropyl)tetramethyldisiloxane (Fig. 1).

## Results and discussion

### Synthesis and characterisation

By addition of a methanolic solution of  $\text{Fe}(\text{NCS})_3$ , obtained by reacting  $\text{Fe}(\text{ClO}_4)_3 \cdot 6\text{H}_2\text{O}$  with  $\text{KNCS}$ , after separation of partly precipitated  $\text{KClO}_4$  from the solution, to the *in situ* prepared  $\text{H}_4\text{L}$  (Fig. 1) the complex  $[\text{Fe}_7(\text{H}_2\text{L})_6(\text{NCS})_6](\text{ClO}_4)_3 \cdot 10\text{H}_2\text{O}$  (**1**) was isolated with 25% yield. The doubly deprotonated ligand contains two rigid salicylidene moieties, each decorated with a  $\text{COOH}$  group, and separated by a long flexible aliphatic chain with a central tetramethyldisiloxane unit. Complex **1** is not soluble in water, methanol and other organic solvents preclud-

<sup>a</sup>“Petru Poni” Institute of Macromolecular Chemistry, Aleea G. Ghica Voda 41A, 700487 Iasi, Romania. E-mail: shova@icmpp.ro

<sup>b</sup>Laboratoire National des Champs Magnétiques Intenses-CNRS, Université Joseph Fourier, 25 Avenue des Martyrs, 38042 Grenoble Cedex 9, France

<sup>c</sup>Regional Centre of Advanced Technologies and Materials, Faculty of Sciences, Palacký University in Olomouc, Šlechtitelů 11, 78371 Olomouc, Czech Republic

<sup>d</sup>Institute of Inorganic Chemistry of the University of Vienna, Währinger Strasse 42, A-1090 Vienna, Austria. E-mail: vladimir.arion@univie.ac.at

† Electronic supplementary information (ESI) available: Experimental details, supplementary tables and figures. CCDC 1520203. For ESI and crystallographic data in CIF or other electronic format see DOI: 10.1039/c7dt00141j

ing any characterisation in solution by optical spectroscopy and ESI mass spectrometry. Therefore, it was investigated in the solid state by IR, single crystal X-ray diffraction, Mössbauer spectroscopy and temperature dependent magnetic susceptibility measurements.

Single-crystal X-ray crystallography revealed that **1** crystallizes in the cubic space group  $Ia\bar{3}$  and has an ionic crystal structure built up from heptanuclear cations  $[\text{Fe}_7(\text{H}_2\text{L})_6(\text{NCS})_6]^{3+}$  and  $\text{ClO}_4^-$  anions. The asymmetric part and the overall structure of the complex cation are shown in Fig. 2 and 3, respectively. The polynuclear cation (Fig. 3) has its own  $S_6$  point group symmetry and adopts a hexagonal arrangement of the wheel's iron(III) atoms.

Fe1 occupies a special position on the centre of inversion with  $\text{Fe1}\cdots\text{Fe2}$  and  $\text{Fe2}\cdots\text{Fe2}'$  separations of 5.2387(8) and 5.3895(9) Å, respectively. The Schiff base ligand acts as a doubly deprotonated ligand with two carboxylate groups. The ligand is coordinated in the zwitterionic form where both phenolic hydrogen atoms have moved to the (non-coordinated) aldimine nitrogens N1 and N2 (Fig. 1), as already observed in other systems.<sup>11b</sup> The two carboxylate groups of the Schiff base ligand are both coordinated in  $\mu$ -1,3-bridging mode, but their roles are different. One carboxylate group bridges two neighbouring iron(III) atoms of the wheel's rim, one of which is out of the COO plane by 1.28(5) Å. The second one adopts a *syn-anti* mode of coordination and bridges an iron(III) from the rim with the central iron(III) ion. The latter metal ion adopts a slightly distorted  $\text{O}_6$  octahedral coordination geometry with  $\text{O1-Fe1-O1}'$  ranging from 83.8(1) to 96.2(1)°. The  $\text{N}_1\text{O}_5$  coordination environment of the Fe2 atom is formed by three oxygen atoms of the carboxylate groups, two phenolic oxygen atoms ( $\text{Fe2-O}_{\text{av}} = 1.996(3)$  Å) and a nitrogen atom from a thiocyanate

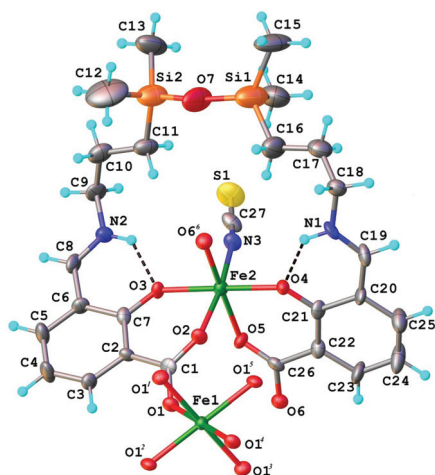


**Fig. 2** ORTEP view of the asymmetric part of the cation  $[\text{Fe}_7(\text{H}_2\text{L})_6(\text{NCS})_6]^{3+}$  with the atom labelling scheme and thermal ellipsoids at the 30% probability level. H-bond parameters:  $\text{N1-H}\cdots\text{O4}$  [N1 H 0.86 Å, H $\cdots$ O4 1.97 Å, N1 $\cdots$ O4 2.604(5) Å, N1-H $\cdots$ O4 130.0°];  $\text{N2-H}\cdots\text{O3}$  [N2 H 0.86 Å, H $\cdots$ O3 1.91 Å, N2 $\cdots$ O3 2.578(6) Å, N2-H $\cdots$ O3 133.1°]. Symmetry codes:  $^1z, x, y$ ;  $^2y, z, x$ ;  $^30.5 - z, 0.5 - x, 0.5 - y$ ;  $^40.5 - x, 0.5 - y, 0.5 - z$ ;  $^50.5 - y, 0.5 - z, 0.5 - x$ .

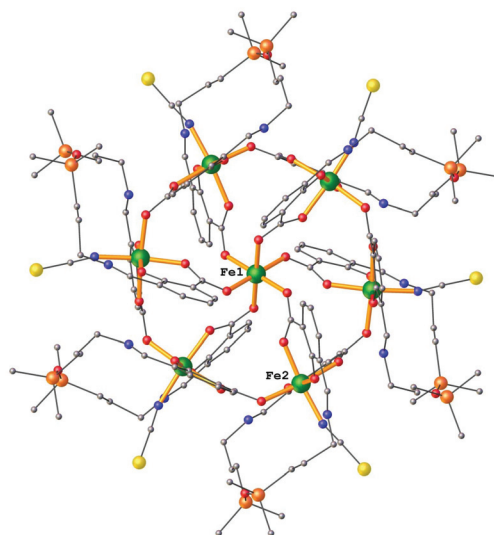


**Fig. 3** View of the cation  $[\text{Fe}_7(\text{H}_2\text{L})_6(\text{NCS})_6]^{3+}$ .

anion ( $\text{Fe2-N3} = 2.019(5)$  Å) ( $\nu_{\text{NCS}}$  at 2051  $\text{cm}^{-1}$ , Fig. S1, ESI<sup>†</sup>). The long flexible siloxane-based linker together with the perchlorate ions ensure a good isolation of the complex cations (Fig. S2, ESI<sup>†</sup>) and the formation of large solvent-accessible voids with a total volume of 52.1% accommodating severely disordered co-crystallised water molecules.

In order to unveil more clearly both oxidation and spin states of the iron ions in **1** we employed zero-field  $^{57}\text{Fe}$  Mössbauer spectroscopy. At 300 K, the  $^{57}\text{Fe}$  Mössbauer spectrum exhibits a clear doublet signature, showing only small signal asymmetry expressed at positive velocity (Fig. 4, upper panel). Analysis of the transmission line revealed the presence of two overlapping doublets, and thus the occurrence of two sets of high spin ( $S = 5/2$ )  $\text{Fe}^{3+}$  cations adopting slightly

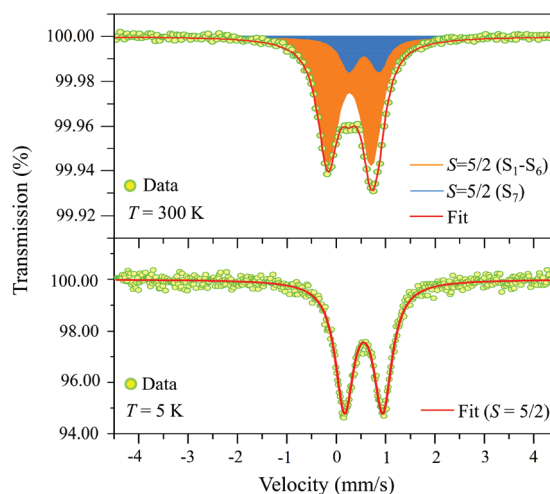


**Fig. 4** Zero-field  $^{57}\text{Fe}$  Mössbauer spectra of **1** recorded at  $T = 300$  K (upper panel) and at  $T = 5$  K (lower panel). The solid lines (orange,  $S_1-S_6$ ; blue,  $S_7$ ) correspond to the spectral components, the red line corresponds to the fitting results. The symbol indicates experimental data.

different coordination environments. The present result mirrors nicely the structural organisation of the iron-wheel complex **1** obtained from X-ray analysis. One doublet encodes the largest relative spectral area (RA of  $84 \pm 0.1\%$ ), and shows an isomer shift ( $\delta$ ) of  $0.30 \pm 0.01 \text{ mm s}^{-1}$  and quadrupole splitting ( $\Delta E_Q$ ) of  $0.82 \pm 0.01 \text{ mm s}^{-1}$ .

The second minor component (RA of  $16 \pm 0.1\%$ ) exhibits a  $\delta$  of  $0.56 \pm 0.01 \text{ mm s}^{-1}$  and a  $\Delta E_Q$  of  $0.61 \pm 0.01 \text{ mm s}^{-1}$ . Therefore, the former doublet can be associated with the six  $\text{Fe}^{3+}$  cations lying on the wheel edge (labeled as  $S_{1-6}$  in Fig. 4 and 5) and the latter with the  $\text{Fe}^{3+}$  cation located on the iron wheel centre (labeled as  $S_7$ ). Upon cooling down to 5 K (Fig. 4, lower panel), the signal asymmetry witnessed at high temperature is lost and the doublet can be fitted with one  $\text{Fe}^{3+}$  ( $S = 5/2$ ) component, encoding a  $\delta$  of  $0.55 \pm 0.01 \text{ mm s}^{-1}$  and a  $\Delta E_Q$  of  $0.78 \pm 0.01 \text{ mm s}^{-1}$ . The isomer shift ( $\delta$ ) and quadrupole splitting ( $\Delta E_Q$ ) extracted from Mössbauer spectroscopy are known to be intimately related to the electron density at the Fe nuclei and hence to reflect subtle differences in the local environment of the iron centre.<sup>12</sup> Since two types of octahedral iron(III) atoms with different environments ( $\text{O}_6$  in  $S_7$  and  $\text{O}_5\text{N}$  in  $S_{1-6}$ ) are present in **1**, two couples of ( $\delta$ ,  $\Delta E_Q$ ) parameters are expected to be needed to interpret the data. This is indeed the case at high temperature reflecting the single-crystal XRD results. Nonetheless, at 5 K, the signal attributed to the outer iron centres merges towards that of the central ion. Accordingly, this loss of asymmetry is ascribed to structural rearrangements around the former ions that increase the electron density at these nuclei. The thermal variation of  $\chi_{\text{M}}T$  for **1** is shown in Fig. 5.  $\chi_{\text{M}}T$  is equal to  $27.36 \text{ cm}^3 \text{ mol}^{-1} \text{ K}$  at 300 K, decreasing upon cooling and reaching a value equal to  $6.50 \text{ cm}^3 \text{ mol}^{-1} \text{ K}$  at 2 K. The  $\chi_{\text{M}}T$  value at room temperature is lower than that expected for seven isolated  $\text{Fe}^{3+}$  ions with  $g = 2$  ( $30.65 \text{ cm}^3 \text{ mol}^{-1} \text{ K}$ ). Such behaviour indicates the presence of dominant antiferromagnetic interactions in **1**. From the X-ray

analysis, the heptanuclear core in **1** can be disentangled by a set of two magnetically non-equivalent  $\text{Fe}^{3+}$  ions ( $S_{1-6}$  and  $S_7$ , see exchange pathways as the inset diagram in Fig. 5). Assuming equivalent (symmetrical/hexagonal) arrangement of the six peripheral iron ions around the central one, in accord with the  $S_6$  point group symmetry found by X-ray diffraction and Mossbauer analysis at 5 K, the magnetic interactions within the  $\text{Fe}_7$  cluster can be analysed with the following isotropic spin Hamiltonian:<sup>13</sup>

$$H = -J_1 \sum_{\substack{ij=1 \\ i \neq j}}^6 S_i S_j - J_2 S_7 \sum_{i=1}^6 S_i$$

with  $S_i = 5/2$ .

The best set of fitting parameters gave  $J_1 = -1.00 \text{ cm}^{-1}$ ,  $J_2 = -1.46 \text{ cm}^{-1}$  and a  $g$  value of 1.95 which correspond to the anti-ferromagnetic interaction *via* two types of carboxylate bridges. The low values of  $J$  parameters imply that multiple spin states are populated even at low temperatures. In addition, given the triangular arrangement of the spins and that the values of  $J_1$  and  $J_2$  are close, some spin frustration is expected to occur at low temperatures (2–5 K). These two statements are confirmed by the difficulty to saturate the magnetisation with an applied field of 5 T at 2 K (Fig. S3, ESI†). Due to the absence of the well-defined ground state and the weak anisotropy (ZFS) expected for iron(III), the compound did not exhibit any out-of-phase ac susceptibility neither in zero dc field nor at 2000 Oe (Fig. S4†).

The solid state EPR spectrum of **1** recorded at 123 K is shown in Fig. 6 and its overall resonance envelope further supports exchange interactions being active among the ferric cations. It exhibits a weak component at  $g = 4.3$ , which is attributed to the middle Kramer doublet ( $|\pm 3/2\rangle$ ) of high spin  $\text{Fe}^{3+}$  cations ( $S = 5/2$ ,  $E/D = 0.33$ ), together with a strong and isotropic component at  $g = 2.00$ , which is the footprint of anti-ferromagnetically coupled ferric centres with non-vanishing moment.

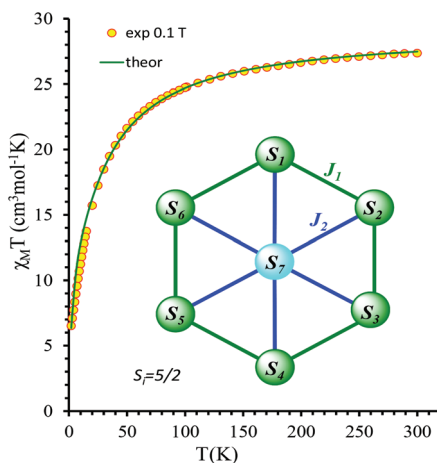


**Fig. 5**  $\chi_{\text{M}}T$  versus  $T$  plot for **1**. The solid line is the best simulation fit according to the spin Hamiltonian model described in the text. The structural sketch shows the relevant exchange interaction pathways ( $J_1$  and  $J_2$ ) present in **1** according to the model.

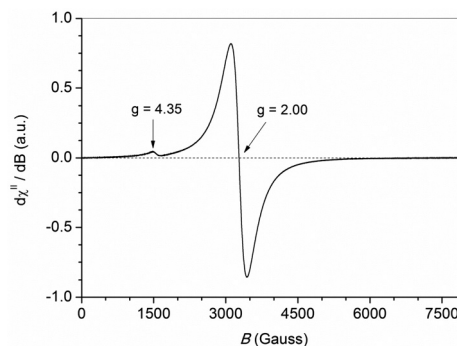


**Fig. 6** The solid line is the EPR powder spectrum of **1**. The sample was air-evacuated inside the EPR tube and saturated with nitrogen prior to measurement. Experimental conditions: 9.144 GHz frequency, 100 kHz modulation frequency, 5 Gauss modulation width, 400  $\mu\text{W}$  microwave power, 8 min sweep time, 0.03 s time constant, 2 scan accumulated and averaged,  $T = 123 \text{ K}$ .

## Conclusions

A Schiff base, which combines two salicylidene moieties with potential bridging carboxylic functionalities in the *ortho*-position to the phenolate group, bridged by a long and flexible aliphatic chain with a central disiloxane moiety, proved to be a powerful tool for assembly of a  $\{\text{Fe}\}_6$  wheel, in the centre of which a seventh iron(III) atom is hosted. Both aldimine groups are protonated and not involved in coordination to iron(III). The presence of the  $\text{NCS}^-$  co-ligand is required to complete the coordination sphere of wheel's iron(III) atoms. The siloxane-based linker ensures a very good isolation of the  $\text{FeC}\{\text{Fe}\}_6$  wheels. X-ray diffraction and Mossbauer spectroscopy indicate that the wheel is very symmetrical down to 5 K. The magnetic susceptibility was therefore reproduced with two meaningful exchange interaction parameters along the rim ( $J_1 = -1.00 \text{ cm}^{-1}$ ) and the radius ( $J_2 = -1.46 \text{ cm}^{-1}$ ) of the wheel. Given the versatility of the salen-type Schiff base family, this work provides the opportunity to vary the metal ions inserted in the wheels and/or to finely tune their magnetic properties. In particular, the modification of the nature of the exchange interaction and/or the increase of ZFS can lead to new metallic wheels with potential SMM behaviour.

## Experimental

### Materials and methods

All starting materials were purchased from Sigma-Aldrich and Acros Organics and used as received unless specified otherwise. Elemental analyses were performed at the Microanalytical Laboratory of the University of Vienna with a Perkin Elmer 2400 CHN Elemental Analyser. The temperature dependence of magnetic susceptibility (2–300 K) was measured on the powdered sample using a SQUID magnetometer (Quantum Design MPMS-XL), applying a magnetic field of 0.1 T. Magnetisation measurements on the same sample have been performed in the absence or presence of the magnetic field (0–5 T) at 2, 3, 4 and 5 K. All data were corrected for the contribution of the sample holder and the diamagnetism of the samples estimated from Pascal's constants.<sup>14,15</sup> Magnetic data analysis was carried out by calculations of energy levels associated with the relevant isotropic spin Hamiltonian by using the MAGPACK program package.<sup>16</sup> The ac magnetic susceptibility was measured at 2 K with an oscillating field magnitude of 3.0 Oe and the frequency ranging between 1 and 1488 Hz. The FTIR spectrum (Fig. S1†) was recorded with 32 scans per spectrum at a resolution of  $4 \text{ cm}^{-1}$  using a Nicolet Fourier Transform Infra-Red (FTIR) spectrophotometer iS 50 IR. Transmission  $^{57}\text{Fe}$  Mössbauer spectra of **1** (iron wheel) were recorded by employing a Mössbauer spectrometer operating in a constant acceleration mode and equipped with 50 mCi  $^{57}\text{Co}$  (Rh) source. While the source was kept at room temperature, the sample was placed inside the chamber of the cryomagnetic system (Oxford Instruments). The sample was measured at 300 K and at 5 K in a parallel direction with respect to the

propagation of  $\gamma$ -rays. The acquired Mössbauer spectrum at 300 K was obtained after 700 h of acquisition time and the spectrum at 5 K was obtained after 168 h; both spectra were processed using the MossWinn software program. The isomer shift values refer to the  $\alpha$ -Fe foil sample at room temperature. The EPR spectrum of **1** was recorded on a JEOL JES-X-320 operating at X-band frequency, equipped with variable temperature control ES 13060DVT5 apparatus.

### Crystallographic structure determination

X-ray diffraction data were collected using an Oxford-Diffraction XCALIBUR E CCD diffractometer with graphite-monochromated  $\text{Mo-K}\alpha$  radiation. The crystal was placed 50 mm from the CCD detector and 72 frames were measured each for 200 s over  $0.75^\circ$   $\omega$ -scan width. The unit cell determination and data integration were carried out using the CrysAlis package of Oxford Diffraction.<sup>17</sup> The structure was solved by direct methods using Olex2 software<sup>18</sup> with the SHELXS structure solution program and refined by full-matrix least-squares on  $F^2$  with SHELXL-97.<sup>19</sup> All H atoms attached to carbon atoms were introduced in idealised positions ( $d_{\text{CH}} = 0.96 \text{ \AA}$ ) using the riding model with their isotropic displacement parameters fixed at 120% of their riding atom. Positional parameters of the H attached to N atoms were obtained from difference Fourier syntheses and verified by the geometric parameters of the corresponding hydrogen bonds. Crystallographic analysis has revealed the structure to contain  $36547.3 \text{ \AA}^3$  (52.1%) of solvent accessible volume per unit cell, which accommodates severely disordered co-crystallised water molecules. The amount of water was determined from elemental analyses, including oxygen determination, but their crystallographic positions could not be reliably localised. Therefore, the “Use solvent mask” subroutine available in the Olex2 program was applied to remove the scattering associated with these disorder guest molecules. As the result of this treatment, the value of  $R_{\text{obs}}$  has been considerably reduced from 0.131 to 0.076. Crystallographic details for the studied structure are provided in Table S1,† while selected bond lengths and angles are listed in Table S2.†

### Synthesis of $[\text{Fe}_7(\text{H}_2\text{L})_6(\text{NCS})_6]\cdot 10\text{H}_2\text{O}$ (**1**)

A mixture of 1,3-bis(3-aminopropyl)tetramethyldisiloxane (0.25 g, 1.0 mmol) and 3-formylsalicylic acid (0.332 g, 2.0 mmol) in methanol (20 ml) was stirred at  $60^\circ\text{C}$  until complete dissolution. Separately, the synthesis of  $\text{Fe}(\text{NCS})_3$  has been performed by mixing  $\text{Fe}(\text{ClO}_4)_3$  (0.44 g, 1.18 mmol) with KNCS (0.115 g, 1.18 mmol) in methanol (10 ml). The precipitate of  $\text{KClO}_4$  formed was separated by filtration, and the filtrate was added dropwise to the *in situ* prepared solution of the Schiff base. The resulted mixture was refluxed for 20 min and filtered. Then MeCN (7 ml) was added and the solution was allowed to stand at room temperature producing red crystals, which were separated after 24 h, washed with a mixture of MeOH/MeCN 2 : 1 (3 ml) and dried in air. Yield: 0.19 g, 25.3%. Anal. Calcd for  $\text{C}_{162}\text{H}_{224}\text{Fe}_7\text{Cl}_3\text{N}_{18}\text{O}_{64}\text{S}_6\text{Si}_{12}$  ( $M_r$  4474.29), %: C, 43.49; H, 5.05; N, 5.63; S, 4.30; O, 22.89.

Found, %: C, 43.21; H, 91; N, 5.68; S, 4.14; O, 22.45. IR,  $\text{cm}^{-1}$ : 3426, 3074, 2953, 2051, 1658, 1609, 1560, 1458, 1234, 877, 838, 796, 765, 653.

## Acknowledgements

S. S. is thankful to the Marie Skłodowska-Curie Research and Innovation Staff Exchange Programme (H2020-MSCA-RISE-2016, project number 734322-SPINSWITCH) for financial support of this work.

## References

- 1 K. L. Taft and S. J. Lippard, *J. Am. Chem. Soc.*, 1990, **112**, 9629–9630.
- 2 (a) S.-J. Liu, S.-D. Han, J.-M. Jia, L. Xue, Y. Cui, S.-M. Zhang and Z. Chang, *CrystEngComm*, 2014, **16**, 5212–5215; (b) E. M. Rumberger, L. N. Zakharov, A. L. Reingold and D. N. Hendrickson, *Inorg. Chem.*, 2004, **43**, 6531–6533; (c) T.-Z. Zhang, Z.-M. Zhang, Y. Lu and E.-B. Wang, *J. Coord. Chem.*, 2012, **65**, 48–54; (d) J. Fielden, M. Speldrich, C. Besson and P. Kögerler, *Inorg. Chem.*, 2012, **51**, 2734–2736; (e) R. W. Saalfrank, I. Bernt, M. M. Chowdhry, F. Hampel and G. B. M. Vaughan, *Chem. – Eur. J.*, 2001, **7**, 2765–2769; (f) R. W. Saalfrank, C. Deutscher, S. Sperner, T. Nakajima, A. M. Ako, E. Uller, F. Hampel and F. W. Heinemann, *Inorg. Chem.*, 2004, **43**, 4372–4382; (g) R. W. Saalfrank, C. Deutscher, H. Maid, A. M. Ako, S. Sperner, T. Nakajima, W. Bauer, F. Hampel, B. A. Heß, N. J. R. van Eikema Hommes, P. Ralph and F. Heinemann, *Chem. – Eur. J.*, 2004, **10**, 1899–1905; (h) M. Murugesu, K. A. Abboud and G. Christou, *Dalton Trans.*, 2003, 4552–4556.
- 3 (a) L. F. Jones, A. Batsanov, E. K. Brechin, D. Collison, M. Helliwell, T. Mallah, E. J. L. McInnes and S. Piligkos, *Angew. Chem., Int. Ed.*, 2002, **41**, 4318–4321; (b) C. Cañada-Vilalta, T. A. O'Brien, M. Pink, E. R. Davidson and G. Christou, *Chem. Commun.*, 2003, 1240–1241; (c) C. Cañada-Vilalta, T. A. O'Brien, M. Pink, E. R. Davidson and G. Christou, *Inorg. Chem.*, 2003, **42**, 7819–7829; (d) S. G. Baca, S. Breukers, A. Ellern and P. Kögerler, *Acta Crystallogr., Sect. C: Cryst. Struct. Commun.*, 2011, **67**, m371–m374; (e) N. Ahmed, A. Upadhyay, T. Rajeshkumar, S. Vaidya, J. Schnack, G. Rajaraman and N. Shanmugam, *Dalton Trans.*, 2015, **44**, 18743–18747.
- 4 (a) K. L. Taft, C. D. Delfs, G. C. Papaefthymiou, S. Foner, D. Gatteschi and S. J. Lippard, *J. Am. Chem. Soc.*, 1994, **116**, 823–832; (b) C. Benelli, S. Parsons, G. A. Solan and R. E. P. Winpenny, *Angew. Chem., Int. Ed. Engl.*, 1996, **35**, 1825–1828; (c) G. Jiang, Y. Li, W. Hua, Y. Song, J. Bai, S. Li, M. Sheer and X. You, *CrystEngComm*, 2006, **8**, 384–387.
- 5 (a) C. R. Raptopoulou, V. Tangoulis and E. Devlin, *Angew. Chem., Int. Ed.*, 2002, **41**, 2386–2389; (b) A.-A. H. Abu-Nawwas, J. Cano, P. Christian, T. Mallah, G. Rajaraman, S. J. Teat, R. E. P. Winpenny and Y. Yukawa, *Chem. Commun.*, 2004, 314–315.
- 6 (a) S. P. Watton, P. Fuhrmann, L. E. Pence, A. Caneshi, A. Cornia, G. L. Abbati and S. J. Lippard, *Angew. Chem., Int. Ed. Engl.*, 1997, **36**, 2774–2776; (b) P. King, T. C. Stamatou, K. A. Abboud and G. Christou, *Angew. Chem., Int. Ed.*, 2006, **45**, 7379–7383.
- 7 H.-C. Yao, J.-J. Wang, Y.-S. Ma, O. Waldmann, W.-X. Du, Y. Song, Y.-Z. Li, L.-M. Zheng, S. Decurtins and X.-Q. Xin, *Chem. Commun.*, 2006, 1745–1747.
- 8 (a) A. K. Powell, S. L. Heath, D. Gatteschi, L. Pardi, R. Sessoli, G. Spina, F. Del Giallo and F. Pieralli, *J. Am. Chem. Soc.*, 1995, **117**, 2491–2502; (b) Z.-M. Zhang, S. Yao, Y.-G. Li, R. Clérac, Y. Lu, Z.-M. Su and E. B. Wang, *J. Am. Chem. Soc.*, 2009, **131**, 14600–14601; (c) Z.-M. Zhang, Y.-G. Li, S. Yao, E.-B. Wang, Y.-H. Wang and R. Clérac, *Angew. Chem., Int. Ed.*, 2009, **48**, 1581–1584.
- 9 N. Hoshino, A. M. Ako, A. K. Powell and H. Oshio, *Inorg. Chem.*, 2009, **48**, 3396–3407.
- 10 H. Zhang, J. Zhang, R. Liu, Y. Li, W. Liu and W. Li, *Eur. J. Inorg. Chem.*, 2016, 4134–4144.
- 11 (a) A. Soroceanu, M. Cazacu, S. Shova, C. Turta, J. Kožiček, M. Gall, M. Breza, P. Rapta, T. C. O. MacLeod, A. J. L. Pombeiro, J. Telser, A. Dobrov and V. B. Arion, *Eur. J. Inorg. Chem.*, 2013, 1458–1474; (b) M. Alexandru, M. Cazacu, A. Arvinte, S. Shova, C. Turta, B. C. Simionescu, A. Dobrov, E. C. B. A. Alegria, L. M. D. R. S. Martins, A. J. L. Pombeiro and V. B. Arion, *Eur. J. Inorg. Chem.*, 2014, 120–131; (c) M.-F. Zaltariov, M. Alexandru, M. Cazacu, S. Shova, G. Novitchi, C. Train, A. Dobrov, M. V. Kirillova, E. C. B. A. Alegria, A. J. L. Pombeiro and V. B. Arion, *Eur. J. Inorg. Chem.*, 2014, 4946–4956; (d) M. Cazacu, S. Shova, A. Soroceanu, P. Machata, L. Bucinsky, M. Breza, P. Rapta, J. Telser, J. Krzystek and V. B. Arion, *Inorg. Chem.*, 2015, **54**, 5691–5706.
- 12 P. Gütllich and J. Ensling, *Inorganic Electronic Structure and Spectroscopy*, John Wiley & Sons, New York, 1999, vol. I, pp. 161–211.
- 13 M. Menelaou, E. Vournari, V. Psyharis, C. P. Raptopoulou, A. Terzis, V. Tangoulis, Y. Sanakis, C. Mateescu and A. Salifoglou, *Inorg. Chem.*, 2013, **52**, 13849–13860.
- 14 G. A. Bain and J. F. Berry, *J. Chem. Educ.*, 2008, **85**, 532–536.
- 15 O. Kahn, *Molecular Magnetism*, VCH Publishers, Inc., New York, Weinheim, Cambridge, 1993.
- 16 J. J. Borrás-Almenar, J. M. Clemente-Juan, E. Coronado and B. S. Tsukerblat, *J. Comput. Chem.*, 2001, **22**, 985–991.
- 17 *CrysAlis RED*, Version 1.171.34.76, Oxford Diffraction Ltd, 2003.
- 18 O. V. Dolomanov, L. J. Bourhis, R. J. Gildea, J. A. K. Howard and H. Puschmann, *J. Appl. Crystallogr.*, 2009, **42**, 339–341.
- 19 G. Sheldrick, *Acta Crystallogr., Sect. A: Fundam. Crystallogr.*, 2008, **64**, 112–122.